Membrane Technology

ISSN (online): 1873-4049

Application of Static State Estimator in Boilers of Thermal Power Stations

Hamed Shaker[1*], Ahmed Al Rajihy[2]

[1,2] Department of Mechanical Engineering, University of Kerbala

College of Mechanical Engineering, University of Kerbala

[*]Email: hamed.s@s.uokerbala.edu.iq

Abstract

Controlling bad data is one of the most important challenges in power systems because it affects the continuity of plants operation in an appropriate way. Bad data can appear morely in the control center of thermal power plants due to the malfunctioning of sensors which feeding the central processing unit (CPU) through wireless or cables communication system. The happened malfunctioning is because of the harsh environment especially in the boiler sections where an elevated temperature results due to fuel combustion. The bad data may cause inaccurate decisions from the central unit which may lead to sudden shutdowns of the overall station. The sudden shutdown results in losses in the generation of electrical energy where restarting the station requires long time to reach steady state operation. The bad data can be treated by an estimator based on suitable mathematical model. In this paper an estimator is presented to treat the bad data received from the boiler of the thermal power stations. The mathematical model of the estimator is written to simulate the boiler system based on heat transfer principles. The weighted least squares algorithm technique (WLS) is selected to execute the state estimator. The effectiveness of the estimator is tested by inserting white noise and bad data. The results show that the estimator is effective where it can identify bad data. The presented estimator is applied on the boiler of Al-Doura in Baghdad thermal station as a case study, due to the low performance of metering system of this plant. The results show that the estimator can detect and identify even to 10 bad data in the same time at a redundancy ratio of 2.125.

Keywords: Boiler Construction, Simulation of Boiler, State Estimation, Mathematical Model, Numerical Analyses

1. Introduction

Thermal power plants (TPPs) provide the majority of the world's energy delivery using conventional fuels including coal, gas, fuel oil, and even crude oil [1]. Thermal power plants depend on Rankine thermodynamic cycle, which is represented by the schematic diagram shown in Figure (1). The cycle includes generating steam in a steam generator (boiler) and expanding the steam through a turbine which convert the kinetic energy of the expanded steam to mechanical energy as a torque at certain speed. The turbine is coupled to an electrical generator which has the ability to convert the mechanical energy to electrical energy. In general, the efficiency of thermal power stations is a measure of plants performance. A power plant's efficiency is often represented as a percentage based on the ratio of its electrical output to the quantity of heat generated by fuel combustion. The typical efficiency range for commercial plants lie between 30% and 65% [1]. The initial enormous construction costs, operational complexity, maintenance issues, complex and nonlinear behavior, interaction with the power distribution grid, operation in extremely harsh temperatures encourages clear enhancements in thermal power stations. The enhancements include materials, processes, operational procedures, maintenance and evaluation techniques, simulation of thermal behavior, and root cause failure analysis [2]. The boiler of thermal power plants is made up of different sections which are working together to convert the chemical energy of the fossil fuel to heat energy [3] in the steam at proper pressure and temperature. Drum type boiler is a large, complex heat exchange units designed capacity to produce steam at high temperatures and pressures. These boilers are often water tube boilers, that is the water circulates through a number of suitable tubes. Figure (2) illustrates the boiler sections and successive of processes.

ISSN (online): 1873-4049

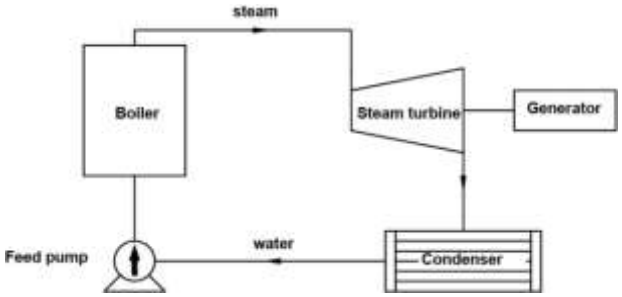

Figure 1. The Mechanism of Rankine Cycle

- The water wall tubes (Risers) is composed of several vertical tubes imposed at the internal side of the four walls of the furnace, which produces saturated steam at 360 ºC [2].
- The drum is a big thick cylindrical vessel that is approximately half filled with water used to separate the steam from the steam-water mixture coming from the risers.[4]
- The economizer is installed to increase the efficiency of the plant by recovering waste heat from flue gases leaves the thermal power plant [5, 6].
- Superheaters are composed from banks used to superheat the saturated steam to about 540 ºC.
- Reheaters is a bank of tubes used to reheat the steam that leaves the first and/or second stage of turbines in order to eliminate steam moisture and increasing plant efficiency.[6]

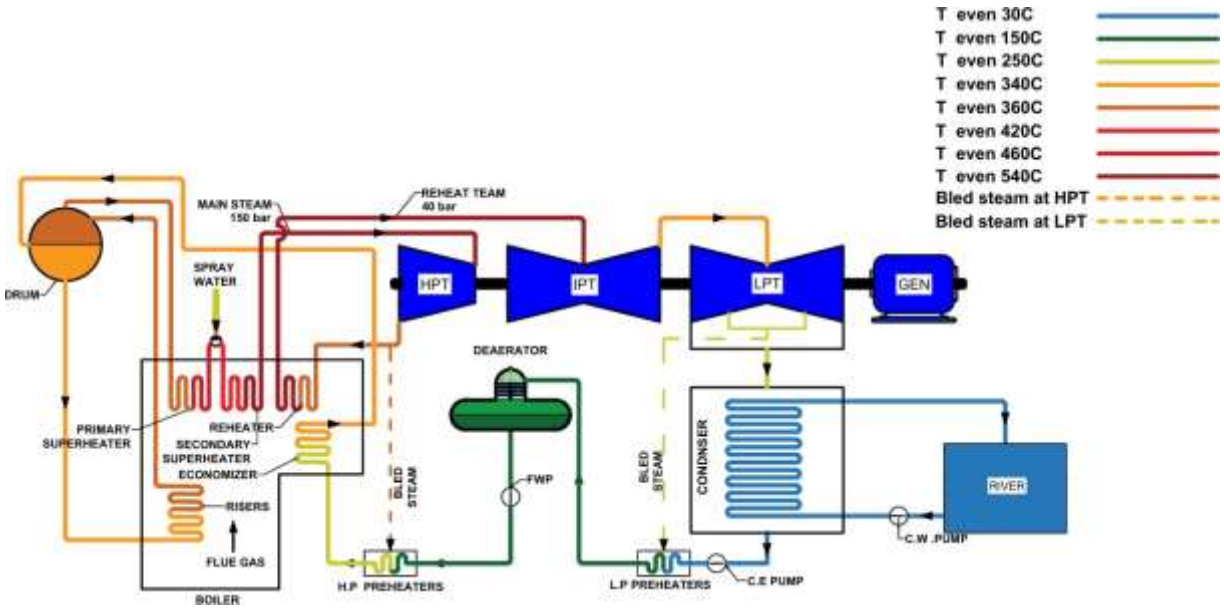

Figure 2. Al-Doura thermal power plant diagram

The problem of simulating the boiler in thermal power plants, and presenting state estimators was investigated by many researchers. Here we will site a few which related to our problem.

K. L. LO and Z. M. SONG (1990) [7] explained the overall structure of the computer simulation, as well as the estimating technique for a static-state estimator, for a power station boiler. The created estimator was based on a mathematical model. The estimator is observable, according to an analysis of the observability of measurement equations. The weighted least squares approach-based estimator was evaluated in a random noise setting. The numerical results show that the estimator performs effectively with redundancy ratio of 2.35.

The estimator presented by K.L. Lo et al (1990) [8] was applied to a 250 MW double-flow, single-reheat steam turbine with seven feedwater heaters. They show that the test results demonstrate that the estimator operates effectively across a wide range of measurement errors and redundancy ratio of 2.3.

The research prepared by Carlos Expedite Bandak (2013) [9] covered the broad framework for state estimation in power systems. Additionally, it covered standard methods for dealing with both linear and non-linear systems, one of which the (WLS) was demonstrated with various numerical examples. The research on state estimate for a Permanent Magnet Synchronous Motor utilizing various techniques is the last section of the paper. A quick comparison of the outcomes from using these approaches and a contrast of their performances round up the study. The author showed that the weighted least square (WLS) technique, the most popular and well-known approach, is quite helpful in the field of power engineering.

T P Vishnu et al (2015) [10] described the Weighted Least Squares static state estimate method of an electric power system. Static state estimate performed using data made accessible by the SCADA system. This research uses data gathered by Newton Raphson Load flow analysis. The weighted least squares approach evaluates the condition of the power system using the weights assigned to each measurement. A state estimator should be able to detect and identify the existence of invalid data. If bad data is included in the measurements, the estimated state variables will differ from actual state variables. This solution makes use of an existing SCADA system and hence is simple to install. When compared to other procedures, this technique is not particularly robust. However, this approach may be used with the phasor measurement unit (PMU) based state estimation methodology to achieve a more robust result.

Majdoub Meriem et al (2016) [11] investigated how the effectiveness of WLS state estimation changes as a function of four parameters; number of measures, measurement type, measurement weight, and noise level. Different tests were evaluated on the 3-bus and IEEE 14-bus systems. The results showed that accurate system state estimates can be obtained with a minimum of measurement data by the condition of selecting a good combination of accurate measurements. The simulations demonstrated that higher redundancy increases estimate accuracy, but the impact is not uniform. The research of the influence of measurement weights and noise shows that both elements must be integrated to produce the best estimate. Indeed, the most accurate measurements (with lower noise levels) should be given more weight than bad ones (with high noise levels).

Aleksandar Jovicic1 and Gabriela Hug1 (2020) [12] were concerned with the issue of removing bad data and transmission line faults from power system estimators. Techniques for picking suspected bad data and line errors for a residual search operation are discussed, as well as tested results for buses IEEE 14, 57, and 118, as well as the 2869 and 13659 test systems, are used to assess the performance of the suggested algorithm. The collected results show that the suggested technique has a minimal computational load and extremely good accuracy. Additionally, the largest normalized residual (LNR) test, which makes the method robust against bad data, may be used with the WLS framework and has a low computational cost because of the estimate stage's linearity.

Andi Nur Putri et al (2020) [13] studied and analyzed the results of Remote Terminal Unit measurements and detect bad data on the bus using State Estimation. The study was carried out in the Load Control Unit of (South, Southeast, and West Sulawesi, hereafter SULSELRABAR). The data utilized in the analysis were channel impedance data and remote terminal units (RTU) measurement results, which included bus, voltage, Million Volt-Ampere Reactive (MVAR) injection, and load data from SULSELRABAR's electrical system. According to the results, the examination of 35 buses indicated that state estimate using the Weighted Least Squares (WLS) can demonstrate the value of voltage and rotor angle estimation for 30 buses. The largest power flow state estimate error (0.0871) was attained on bus 29. Two buses had error values that above the tolerance: bus 27, with an error of 0.0575, and bus 29, with an error of 0.0871. Measurement inaccuracy or bad measurement can be caused by the interruption of communication from the substation to the control center or the non-calibration of the measuring instruments at the substation, resulting in disinformation at the control center.

I. A. Araga et al (2021) [14] They dealt with the Nigerian 330KV transmission network's problem of inaccurate data readings. This study estimated the actual status of the power system network using the optimal

weighted least squares approach. In order to do this study, mathematical models of the system network were constructed, and the Weighted Least Square estimate approach was used to various weights based on the measurement type. The network's IEEE 14 buses are used for the observability and error quantification procedure. This work runs state estimate simulations and uses the MATLAB computational tools to get significant state results. In comparison to the state estimate result, the estimation technique's findings showed measurement data inaccuracies with a considerable variation of 1.14 of the maximum voltage inaccuracy. The disparity between the

Lalit Kumar & Pooja K. Kherdikar (2022) [15] briefly discussed the essential principles and mathematical models of power system state estimation, as well as the process for detecting, identifying, and eliminating bad data. Research and development of approaches for power system modeling, including mathematical formulation, numerical solutions, computational procedures, measurement kinds, and error detection in the literature. Although the WLS approach is frequently utilized, a well-developed technique for power system state estimate has been shown to be ineffective in the face of repeated bad data. At last, the possibilities for its development trend were suggested based on the state evaluation of the research's existing position.

Hondo, Amina et suggested (2023) [16] an algorithm for estimating the condition of the electrical power system that is based on the weighted least squares (WLS) approach. Results show that the weighted least squares approach offers high accuracy and minimizes error. The state estimation technique in the MATLAB software package was evaluated through simulation on the IEEE 118-bus test system. By creating and testing the best estimation procedure for the state of variables, such as voltages by module and angle in every node of the network, this paper added to the body of knowledge already in existence. This process may prove beneficial for the operation and control of future smart and digitalized electric power systems.

Sheikh and Chetan (2023) [17] in this article described simulated estimation and Weighted Least Square (WLS) estimation methods. With a set of measurements, the method and codes are created and tested in MATLAB for typical IEEE 14 bus systems, and the results seem to be adequate in terms of lowering measurement errors.

The aim of this work is to perform a static state estimator based on the basic principles of heat transfer for the mathematical model of the boiler metering system, and exploiting the weighted least squares algorithm. Al-Doura thermal power station in Baghdad is taken as taken as the application field for this estimator due to the problems in the metering system of this station.

2. Simulation of the Boiler

For the purpose of making a state estimation process for the boiler, a mathematical model should be derived to describe the boiler behavior under steady state conditions. The mathematical model of the boiler must be having the ability of simulation on computer. For steady state estimation operation of steam power plants, the model for on-line state estimation should satisfy two points, the accuracy which should be within prescribed range, and minimum computation time. Therefore, the developed mathematical model should be sufficiently accurate to represent the boiler and sufficiently simple for direct on-line applications. To avoid the complexity and confusion of mathematical model of the boiler of Al-Doura station is divided into seven subsystems according to the construction and function of each subsystem as shown in Figure (3). The subsystems are; economizer, drum, waterwalls, primary superheater, first bank secondary superheater, second bank secondary superheater and the reheater. According to this partition, each section (subsystem) can be treated as a lumped parameter subsystem in which the energy conservation principle is applied to each section to represent the models for the subsystem are coupled to form the overall system model. In general, the following assumptions are made to simplify the complexities of the theoretical analysis [18]:

1. Constant mass flow rate of water and steam in each section.
2. The temperature equality and constancy of mass flow rate between any two adjacent sections is taken as the boundary conditions.
3. All the boiler sections, unless the drum, are considered as ideal heat exchangers.

4. The kinetic and potential energies are neglected in the energy balance equations for each section.

2.1. Modelling of Boiler Measurement System

Any of the boiler measurand variables can be expressed by a suitable measurement equation as a function of state variables. The related measurement equation should give the value of the measurement variable in terms of state variables and system corresponding parameters. The positions of the meters have a significant impact on how the measurement equations are derived. Temperature, pressure, and steam, water & gas mass flow rates are the main quantities recorded by a power plant's measurement system. The measurement variables of Al-Doura boiler are; temperatures, pressures and mass flow rates of steam & water at inlet and outlet of each boiler section, temperature and pressure in the drum as well as the metal temperature of tubes in each boiler section. The measurement equations for each section in the boiler are given in the following sections.

2.1.1. The economizer

The economizer is the section at which the feed water is preheated to improve the efficiency of the power plant. The heat transferred from the flue gases to the feed water through the economizer tubes is proportional to the difference of water enthalpy between inlet and outlet of the tubes which can be stated mathematically as [18]

$$Q_{ec} = M(H_{eco} - H_{eci}) \quad (1)$$

expressing the enthalpy in terms of temperature and specific heat, the state equation, equation (1), can be rewritten as:

$$Q_{ec} = M(C_{eco}T_{eco} - C_{eci}T_{eci}) \quad (2)$$

The rate of heat transfer from tube to the feed water can be represented by the empirical equation [18, 19]

$$Q_{ecmw} = K_{ec1}M^{0.8}(T_{ecm} - T_{eco}) \quad (3)$$

Also, the heat flux from the flue gases passing through the economizer to the tubes given by the relation [18-20]

$$Q_{gecm} = K_{ec2}\, M_g^{0.6}(T_{geo} - T_{ecm}) \quad (4)$$

The values of K_{ec1} and K_{ec2} are given in appendix-B (Table 6) The heat energy given by the flue gas to the tubes is given by

$$Q_{gec} = M_g C_{gec}(T_{geco} - T_{geci}) \quad (5)$$

Under steady state operation condition of the boiler, the following relation can be stated

$$Q_{ec} = Q_{ecmw} = Q_{gecm} = Q_{gec} \quad (6)$$

From the above six equations one can obtain the measurement equations for the economizer metal tube temperature, T_{ecm} , outlet temperature of flue gases, T_{eco} , inlet temperature of flue gases, T_{eci} are presented below respectively [18]

$$T_{ecm} = (1 + \frac{C_{eco}M^{0.2}}{K_{ec1}})\, T_{eco} - \frac{C_{eci}M^{0.2}}{K_{ec1}} T_{eci} \quad (7)$$

$$T_{geco} = [1 + C_{eco} M (\frac{1}{K_{ec2}M_g^{0.6}} + \frac{1}{K_{ec1}M^{0.8}})]\, T_{eco} - C_{eci} M (\frac{1}{K_{ec2}M_g^{0.6}} + \frac{1}{K_{ec1}M^{0.8}})\, T_{eci} \quad (8)$$

$$T_{geci} = [1 + C_{eco} M (\frac{1}{C_{gec}M_g} + \frac{1}{K_{ec2}M_g^{0.6}} + \frac{1}{K_{ec1}M^{0.8}})]\, T_{eco} - C_{eci} M (\frac{1}{C_{gce}M_g} + \frac{1}{K_{ec2}M_g^{0.6}} + \frac{1}{K_{ec1}M^{0.8}})\, T_{eci} \quad (9)$$

2.1.2 Drum and waterwalls

It is basically known that all the saturation properties depend uniquely on the drum pressure, P_{dr} . *If* P_{dr} is given, the temperature of the saturated steam, T_{drs} , the saturated steam enthalpy, H_{drs} , the saturated water enthalpy, H_{drw} , the saturated steam density, ρ_{wos} , and the saturated water density, ρ_{wow} , can be evaluated in terms of drum pressure, P_{dr} . The following equations are derived by fitting the properties taken from steam tables.

ISSN (online): 1873-4049

$$T_{drs} = A_1 P_{dr}^2 + B_1 P_{dr} + C_1 \quad (10)$$

$$H_{drs} = A_2 P_{dr}^2 + B_2 P_{dr} + C_2 \quad (11)$$

$$H_{drw} = A_3 P_{dr}^2 + B_3 P_{dr} + C_3 \quad (12)$$

$$\rho_{wos} = A_4 P_{dr}^2 + B_4 P_{dr} + C_4 \quad (13)$$

$$\rho_{wow} = A_5 P_{dr}^2 + B_5 P_{dr} + C_5 \quad (14)$$

The value of the constants A, B C are defined in Tables (7) and (8) which is given in Appendix-B. The bulk of the heat energy generated in the furnace is absorbed by the working fluid (water) that flowing in the riser tubes. The heat transferred from the riser tubes to the steam water mixture is given the equation [18, 19]:

$$q_{wm} = K_w (T_{wm} - T_{drs})^3 \quad (15)$$

The outlet flow from the riser tubes which entering the drum via the cyclones (steam separators) is a mixture of a saturated steam of density ρ_{wos} and saturated water having density ρ_{wos}. The density of this mixture differs from that of steam and water is denoted by ρ_{wo} . In order to predict the steam quality, x, the relation between the three densities is given by [19]:

$$\frac{1}{\rho_{wo}} = \frac{x}{\rho_{wos}} + \frac{1-x}{\rho_{wow}} \quad (16)$$

In terms of steam quality, x and feed water flow rate M , the mass flow rate in the waterwalls becomes:

$$M_w = \frac{M}{x} \quad (17)$$

where M and M_w are the mass flow rates in the economizer and the waterwalls respectively. Accordingly, the value of x is determined by

$$x = \frac{\frac{1}{\rho_{wo}} - \frac{1}{\rho_{wow}}}{\frac{1}{\rho_{wos}} - \frac{1}{\rho_{wow}}} \quad (18)$$

In other words, by our knowledge of the relationship between the density of both steam and water with the saturation pressure, and by relying on steam tables for a range of pressures and extracting the density values of the water and steam at the saturation pressure for each pressure at a certain value and put them in equation (18) we can derive fitting equation (19), which can be used to calculate the ratio of steam to water directly at the saturation pressure. Pressure range in (bar): $60 \leq P_{dr} \leq 190$

$$x = 8 * 10^{-6} P_{dr}^2 - 6 * 10^{-4} P_{dr} + 0.0497 \quad (19)$$

Where: ρ_{wo} is the average density of the water-steam mixture at the outlet of the waterwalls. The values of ρ_{wos} and ρ_{wow} are calculated by equations (13) and (14) respectively. Because the steam bubbles generated are surrounded by liquid, it is reasonable to expect that all of the vapour will remain saturated. The vast volume of liquid surrounding the steam bubbles prevents the vapour from becoming hotter than the liquid. (In the simulated plant, the mass ratio of vapour to liquid in the waterwalls is always less than about (0.25) [21]. The energy absorbed by steam water mixture inside the waterwalls can calculate by the difference of enthalpy of the saturated steam and that of saturated water as given by the difference equation:

$$Q_w = M_w (H_{drs} - H_{drw}) \quad (20)$$

At steady state, actually there is no net increase of heat energy inside the drum, thus the heat absorbed in waterwalls is equal to the difference between the energy contained in steam leaving the drum to the primary superheater and that contained in the water entering the drum from the economizer [18, 20].

$$Q_w = M(H_{drs} - H_{eco}) \quad (21)$$

If the enthalpy of saturated water is expressed in terms of temperature, T_{drw}, the above equation takes the form

Expressing the enthalpy of the saturated water in terms of temperature, T_{drw}, equation (20) can be rewritten a

$$Q_w = M_w(H_{drs} - C_{drw}T_{drw}) \quad (22)$$

$$Q_w = M(H_{drs} - C_{eco}T_{eco}) \quad (23)$$

From equations (21) and (22) one can calculate the temperature of saturated water in the drum as:

$$T_{drw} = \frac{(M_w - M)}{M_w C_{drw}} H_{drs} + \frac{M}{M_w C_{drw}} H_{eco} \quad (24)$$

$$T_{drw} = \frac{(M_w - M)}{M_w C_{drw}} H_{drs} + \frac{MC_{eco}}{M_w C_{drw}} T_{eco} \quad (25)$$

The heat flux absorbed by the riser tubes is transferred to the steam water mixture and it is given by [18, 20]

$$Q_{wm} = K_w(T_{wm} - T_{drs})^3 \quad (26)$$

In steady state, all the energy absorbed by the riser tubes transferred to steam water mixture and can be represented by the relation;

$$Q_w = Q_{wm} \quad (27)$$

Combining equations (21), (25) according to (26), the following equation is obtained:

$$T_{wm} = \left[\frac{M(H_{drs} - H_{eco})}{K_w}\right]^{\frac{1}{3}} + T_{drs} \quad (28)$$

Writing the enthalpy H_{eco} in therms of T_{eco} and specific heat C_{eco}, this equation will take the form:

$$T_{wm} = \left[\frac{M(H_{drs} - C_{eco}T_{eco})}{K_w}\right]^{\frac{1}{3}} + T_{drs} \quad (29)$$

It is assumed that T_{wm} can be measured, so that equation (29) is one of the measurement equations for the waterwalls section. The drum temperature T_{drs} is also a direct measurement. but it can readily be expressed in terms of P_{dr}

2.1.3. Primary superheater

This section is mounted at the top of the economizer presented by Figure (3). The saturated steam that leaves the drum enters this section and flow through its tubes bank in which heat transferred to tubes by convection. According to assumption number (2). The measurand equation of the temperature of the tube metal of this section, T_{pm} is

$$T_{pm} = \left(1 + \frac{C_{po}M^{0.2}}{K_{p1}}\right) T_{po} - \frac{C_{pi}M^{0.2}}{K_{p1}} T_{pi} \quad (30)$$

This equation with the direct measurement of the temperature at inlet and outlet of the first bank primary superheater, T_{pi}, T_{po} comprise the temperature measurements in this section [18].

ISSN (online): 1873-4049

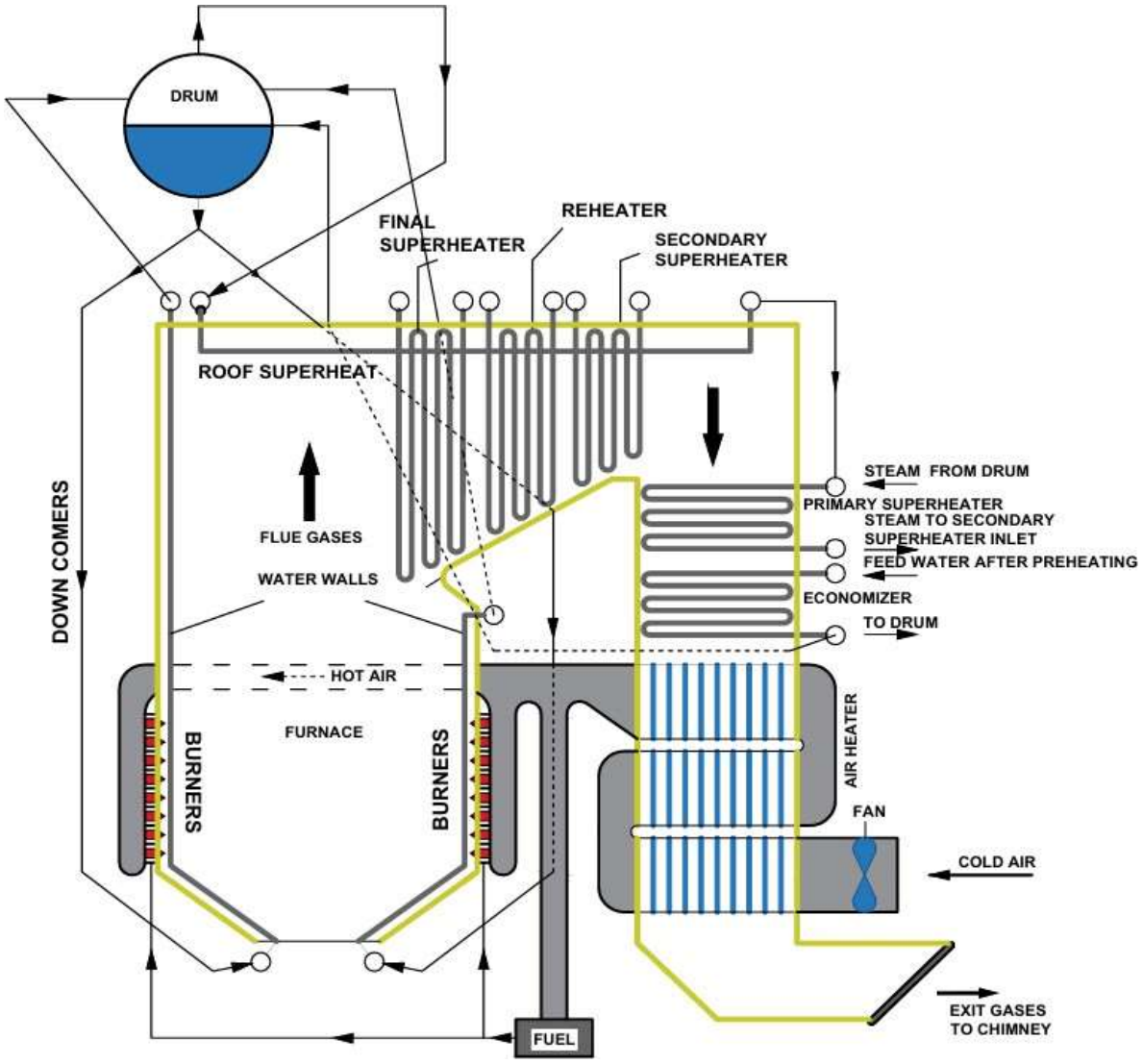

Figure 3. Schematic construction diagram of boiler

2.1.4 First bank secondary superheater

The first bank of secondary superheater is located above the primary superheater as seem in Figure (3). The steam leaving the primary superheater is passed through attemperator by spraying water into the steam to control the temperature of steam from severe levels. The sprayed water is taken from the feed water of the plants especially those working at high level temperatures.

2.1.5. Superheater spray attemperators

Spraying liquid water directly into the steam channel is a common method of controlling steam temperature as shown in Figure (4). The spray mass flow rate is assumed to be 6% of M [18]. For Al-Doura thermal power station there are two stages of attemperators, one located between the primary superheater and the first bank of the secondary superheater, and the other located between the two banks of secondary superheater. that enters the boiler at the inlet of economizer. This process is important to maintain plant efficiency and durability

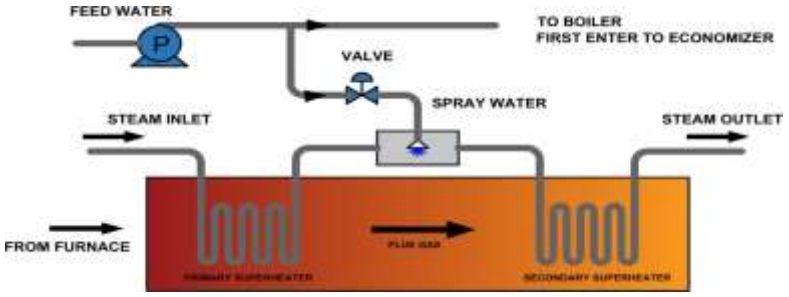

Figure 4. Superheater Spray Attemperator diagram of Al-Doura

The steam mass flowrate in the secondary superheater after the spraying process will be given by

$$M_s = M + M_{sp} \quad (31)$$

The heat flux at 1st bank of secondary superheater inlet is equal to the heat flux from 2nd bank primary superheater outlet plus the spray water at economizer inlet [21] and can be written as

$$q_{s1i} = q_{po} + (q_{ei})_{sp} \quad (32)$$

using the enthalpy relationship equation (32) is written as

$$M_s H_{s1i} = M H_{po} + M_{sp} H_{eci} \quad (33)$$

If the enthalpy of economizer inlet, primary outlet and 1st bank superheat inlet is expressed in terms of temperatures, T_{eci}, T_{po}, T_{s1i} respectively, equation (33) will take the form

$$M_s C_{s1i} T_{s1i} = M C_{po} T_{po} + M_{sp} C_{eci} T_{eci} \quad (34)$$

From equation (33) the temperature of the 1st bank superheat inlet, T_{s1i} can be calculated by the equation

$$T_{s1i} = \frac{MC_{po}}{(M+M_{sp})C_{s1i}} T_{po} + \frac{M_{sp}C_{eci}}{(M+M_{sp})C_{s1i}} T_{eci} \quad (35)$$

The metal tubes' temperature is given by the equation:

$$T_{s1m} = (1 + \frac{C_{s1o}M_S^{0.2}}{K_{s11}})\, T_{s1o} - \frac{C_{s1i}M_S^{0.2}}{K_{s11}} T_{s1i} \quad (36)$$

2.1.6. Second bank superheater

The second bank of secondary superheater is located in front of reheater above the furnace as seen in Figure (3). By the same way of the previous section, the temperature of the 2st bank superheater inlet, T_{s2i} can be calculated as: [18]

$$T_{s2i} = \frac{MC_{s1o}}{(M+M_{sp})C_{s2i}} T_{s1o} + \frac{M_{sp}C_{eci}}{(M+M_{sp})C_{s2i}} T_{eci} \quad (37)$$

The metal tubes' temperature is given by the equation:

$$T_{s2m} = (1 + \frac{C_{s2o}M_S^{0.2}}{K_{s21}})\, T_{s2o} - \frac{C_{s1o}M_S^{0.2}}{K_{s21}} T_{s2i} \quad (38)$$

2.1.7. Reheat

This section, located between the two banks of secondary superheater. This part receives the steam that leaves the high-pressure turbine to raise its temperature before entering the intermediate pressure turbine.

The metal tubes' temperature of this section is [18]

$$T_{rm} = (1 + \frac{C_{ro}M_r^{0.2}}{K_{r1}})\, T_{ro} - \frac{C_{ri}M_r^{0.2}}{K_{r1}} T_{ri} \quad (39)$$

2.1.8. Pressures modelling

The pressure drop of the pressure between the boiler sections is given by a set of empirical equations which represent the pressure measurement equations [18]. These empirical equations are

$$P_{eo} = 0.1P_{ei} + 0.9P_{dr} \quad (40)$$

$$P_{po} = 0.77P_{dr} + 0.23P_{s2o} \quad (41)$$

$$P_{s1i} = 0.48P_{dr} + 0.52P_{s2o} \quad (42)$$

$$P_{s1o} = 0.3P_{dr} + 0.7P_{s2o} \quad (43)$$

In the equations above, every variable on the left-hand side represents a measurable quantity. The location of the corresponding measurement is indicated by the subscript. The drum pressure, P_{dr} , the pressure at the economizer inlet, P_{ei}, and at the second bank of the secondary superheater's outlet, P_{s2o} , are direct measurements as well as the state variables in the model.

3. State Estimation

Throughout the available literature, it seen that the Weighted Least Squares (WLS) approach is powerful for power system state estimation in 1969 [9, 22].

3.1. Static State Estimation

operations can be roughly described as static for the majority of the time, as it is a slowly altering system. Additionally Due to its quasi-static nature, the power system changes slowly over time. The term "static state estimation" (SSE) refers to an estimating method where the state variable is acquired for a given moment in time from the measurement set for that same instant. Compared to the power system, the boiler system appears to benefit more from static-state estimate techniques based on prior experimental findings. A wide variety of measuring sensors been employed to monitor mass flow rates, pressures, and temperatures. The robustness of the estimator needs to be evaluated by testing it with varying bad data (BD) and random noise levels.

3.1.1. Bad data processing

The detecting and identifying measurement errors is the objective of bad data processing. Two categories of measurement errors exist according to the standard deviation, σ [15];

•*Random errors:* $-3\sigma \leq error \leq 3\sigma$

• *Gross errors:* $error \geq 3\sigma$

Meters are prone to random errors that follow statistical distribution. Gross mistakes refer to significant errors in data. Bad data might emerge owing to gross inaccuracies in meters.

3.1.2. weighted least square

The Weighted Least Squares (WLS) technique is a widely utilized approach for power systems state estimation. The goal of state estimate techniques, as this study discusses, is to estimate the state variable as closely as feasible. The idea behind the maximum likelihood principle is to reduce the discrepancy between the estimated value and the real state variable value while increasing the likelihood of approaching the "true" value [9].

3.1.3 State Variable Vector and Measurement Vector

When the boiler operates at the steady state, a set of variables which describe the performance of the metering system are denoted by a state variable. These static state variables describing the boiler metering system are defined as a set of temperatures, set of pressures and set of mass flowrates. The static state variables are represented by the vector [7, 23];

$$\{X\} = \{ \begin{matrix} T_{eci} T_{eco} T_{po} T_{s1o} T_{s2o} T_{ri} T_{ro} P_{eci} \\ P_{dr} P_{s2o} P_{ri} P_{ro} M_r M_f M_a \end{matrix} \}^T \quad (44)$$

The vector given by equation (44) represent the most accurate and trusted measurement points. If the vector $\{X\}$ is defined, all the other interested variables (which are not included in this vector) can be calculated according to the boiler mathematical model given in section 2. The measurements are a set of variables denoted by the vector $\{Z\}$, which correspond to existing metering system of the boiler depending on the practical locations. For the boiler model of Al-Doura thermal power station, the measurement vector $\{Z\}$ is given by the following equation

$$\{Z\} = \begin{Bmatrix} \begin{pmatrix} T_{eci} T_{eco} T_{ecm} T_{geco} T_{geci} T_{drs} T_{drw} T_{wm} \\ T_{pi} T_{po} T_{pm} T_{s1i} T_{s1o} T_{s1m} T_{s2i} T_{s2o} \end{pmatrix}^T \\ T_{s2m} \; T_{ri} \; T_{ro} \; T_{rm} \; P_{eci} \; P_{eco} \; P_{dr} \; P_{po} \\ \{P_{s1i} P_{s1o} \; P_{s2o} P_{ri} P_{ro} \; M \; M_r \; M_f M_a M_{sp}\} \end{Bmatrix} \quad (45)$$

The larger number of variables of the measurement vector gives the larger redundancy. The number of measurements given by equation (45) is 34 and the number of variables of the state vector given by equation (45) is 16, therefor the redundancy is $(\frac{34}{16}) = 2.125$

3.2. Algorithm of Estimator

The actual measurements and the measurement noises may be used to model the measurements; consequently, the measurement process can be expressed as [7, 23, 24]

$$Z = h(X) + e \quad (46)$$

Where: $h(X)$ shows the measurement equations for the 34 non-linearities depends on X.

X is a vector of state variables with 16 dimensions.

e is a noise vector for measurements of 34 dimensions.

Z is a vector that represents all boiler measurements.

By decreasing the sum of the weighted squares of the differences between the measurements and the estimates, the WLS technique achieves its goal. In the case of the non-linear measurement system, the WLS iteratively looks like this [10, 25]

$$\Delta(\hat{X}^k) = G(\hat{X}^k)^{-1} H(\hat{X}^k)^T R^{-1}[Z - h(\hat{X}^k)] \quad (47)$$

$$\hat{X}^{k+1} = \hat{X}^k + \Delta(\hat{X}^k) \quad (48)$$

The iteration count is indicated by the superscript k, and the convergence criteria is provided as

$max|X_i^k - X_I^{k+1}| < \varepsilon$

Where: $H(\hat{X}^k)$ is a Jacobian matrix of dimensions 34 × 16, and its value is obtained by differentiating the $h(\hat{X}^k)$ equation in relation to X at a given position X^0 [23-25]

$$H(\hat{X}^k) = \frac{\partial h(X)}{\partial x} \quad (49)$$

At $\hat{X}(0) = X^o$

The details of the matrix $H(\hat{X}^k)$ are given in Appendix-A [15, 25]

$$G(\hat{X}^k) = H(\hat{X}^k)^T R^{-1} H(\hat{X}^k) \quad (50)$$

G is referred to as the gain matrix in state estimation. Because $\hat{X}$ is modified throughout the iteration process, it is changeable. The diagonal 34 x 34 weighted matrix R entries represent the associated measures' precision. While a small number denotes excellent precision, a big value denotes poor confidence in the associated measurement. Based on estimating theory, the WLS will yield the best unbiased estimate if the weighted component r_i^{-1} is assumed to be the reciprocal of the square of the standard deviation σ_i . The ith element of R is selected as [7]

$$r_i^{-1} = \frac{1}{\sigma_i^2} \quad (51)$$

so that

$$R = r_{ii}^{-1} \quad (52)$$

Where σ is standard deviation [7]

$$\sigma = (a_m Z_t + b_m Z_f) c_m \quad (53)$$

Gaussian distributed random variables with a zero mean and standard deviation σ make up r vector. Equation (53) determines the value of the standard deviation σ.

Where: Z_t represents the measurement's magnitude, which might be mass flow rate, pressure, or temperature.

Z_f corresponds to the meter's full-scale value.

a_m is the measurement value's error coefficient, which is assumed to be 0.02, 0.025, and 0.05 for mass flow rate, pressure, and temperature, respectively. b_m represents the full-scale error coefficient of the meter, which is assumed to be 0.004 for all meters. c_m is the constant, which is assumed to be 1/3 for all meters, that converts the maximum predicted error to the standard deviation. For all measurements, Z_f is defined as $Z_t/0.65$. A gauge's work point is typically between 60% and 70% of its whole scale range [7].

3.2.1 Bad data detection

The Chi-Squares distribution test is one of the techniques used to detect bad data. When bad data are found, they must be identified and eliminated in order to produce an objective state estimate. In terms of the measurement errors, examine the objective function *J*(*x*). The *J-index* is given by the relation [15]

$$r = Z - h(\hat{X}) \quad (54)$$

$$J(x) = \sum_{i=1}^{m} R_{ii}^{-1} (z_i - h(\hat{X}))^2 \quad (55)$$

also, the *J-index* can take another form as [25]

$$J(x) = r^T R^{-1} r \quad (56)$$

Choosing the value from the Chi-square distribution table that corresponds to a detection confidence with $(m - n)$ degrees of freedom and probability Pe (e.g.,99.5%), the following equality is produced [15]

$$Pe = Pr(J(x)) \leq \alpha^2 (m - n), P \quad (57)$$

Where: m represent No. of variables in Z vector

n represent No. of variables in X vector

$\alpha^2 (m - n), Pe$ is threshold denoted by γ

•$(J(x)) - Index$ Test

If $J(x) - Index > \gamma$, there will be suspicions of bad data. If not, it will be presumed that the measures are devoid of bad data. The test threshold at 99.5% confidence level and the degree of freedom $(m - n) = (34 - 16)$, for this case is obtained by MATLAB function $chi2inv$ as follows

$$\gamma = chi2inv(0.995,18) = 37.156$$

3.2.2 Bad data identification

The identification process of bad data can be obtained according to R_w and R_n tests, where both of them depends on the measurement residual. In equation form, these two tests are written as [7]

$$r_i = z_i - h_i(\hat{X}) \qquad i = 1, 2, 3, \ldots \ldots, m \quad (58)$$

The weighted measurements residual is

$$r_{wi} = \frac{z_i - h_i(\hat{x})}{\sigma_i} \qquad i = 1, 2, 3, \dots\dots, m \tag{59}$$

The normalized residual is

$$r_{ni} = \frac{z_i - h_i(X)}{(d_{nii})^{\frac{1}{2}}} \qquad i = 1, 2, 3, \dots\dots, m \tag{60}$$

where d_{ni} is the matrix element that has been diagnosed. [7]

$$D = WR \tag{61}$$

$$W = 1 - H(H^T R^{-1} H)^{-1} H^T R^{-1} \tag{62}$$

Equation (56) serves as the same criteria for detection and it will be employed independently to evaluate each component of the data since the R_w test and the R_n tests are both unique tests. The value of γ corresponding to both r_{wi} and r_{ni} may be found given a false alarm probability Pe , which is commonly set at 0.005. It is assumed that any measurement point, for example the ith measurement, is BD if the above requirement is shown to be greater than the value of γ, otherwise, it is good. It is clear that by reducing the components of equation (58) by each standard deviation, equation. (59) standardizes the measurement residual. As a result, the measurement residual is liberated from the measuring system's error.

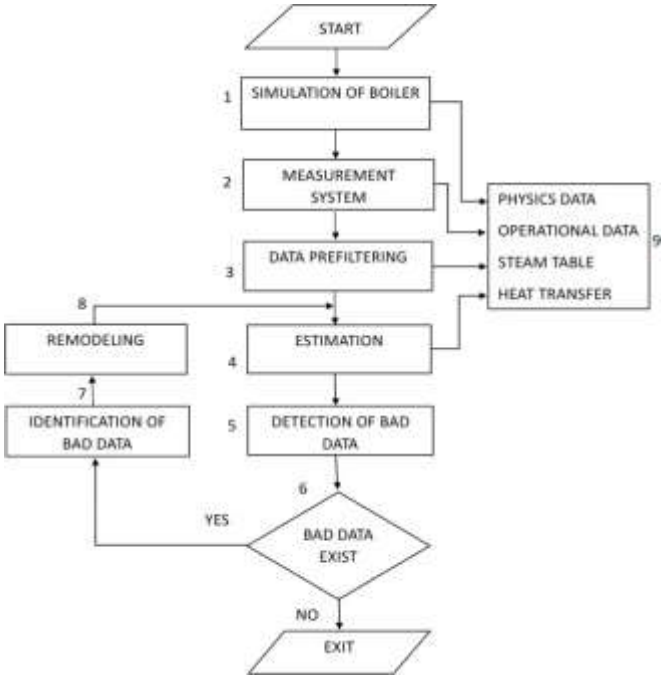

Figure 5. flow chart of estimator construction

3.3 Performance of the Static State Estimator

Two statistical indices, S_e and S_m, are employed to evaluate the performance of the estimator, and they can be represented mathematically as [7].

$$S_e = \left[\frac{1}{m}\sum_{i=1}^{m} \left(\frac{h_i(X) - Z_{ti}}{\sigma_i}\right)^2\right]^{\frac{1}{2}} \tag{63}$$

$$S_m = \left[\frac{1}{m}\sum_{i=1}^{m} \left(\frac{Z_i - Z_{ti}}{\sigma_i}\right)^2\right]^{\frac{1}{2}} \tag{64}$$

where, Z_i is the ith measurement.

$h_i(X)$ is the estimated value.

Z_{ti} is the ith measurement without noise.

S_e and S_m stand for the estimated set's statistical indices and the measurement outcomes, respectively. The estimator is effective in the filtering process $S_e < S_m$.Theoretically, as the number of measurements rises, the value of S_m ought to become closer to unity. In general, the better the estimator in the filtering process, the smaller value of S_e [7].

4. Results and Discussion

The estimator developed for the boiler of Al-Doura power station was tested under Gaussian noises to study its robustness in filtering out the noises. Table 1 presents the results of the estimator under 50% load conditions where the results generated according to equation (46). The value of the two indices ratio (s_e/s_m) is found to be 0.666 (less than one), which indicates that the estimator works well. In table 1, columns 5 and 7 show the discrepancy between the simulation and measurand values and that between simulation and estimated values respectively. Both columns show that the discrepancy lies within 5.547 percent which is an acceptable ratio. The *J-index* was found to be within 18.795 which is lies within the threshold. The robustness of the estimator in detecting, identifying and replacing the bad data is tested by inserting bad data instead of the actual metering readings for different variables. In table 2 T_{drw} was fed as (0ºC) instead of 282.576 ºC as a single bad data, and the estimated value is 286.170 ºC which it is very close to the actual reading. The value of the J-index was 9.747 which means that the estimated values are close to the actual readings. Tables 3 and 4 show 4 and 10 bad data, respectively, were fed instead of the readings received from the metering system. The bad data in both tables are taken as zeros, larger and less than the metering reading. The estimator abled succeed to replace the all the bad data by estimated values. It seen that all the 4 and 10 estimated values are very close to the actual readings.

Table 1 . state estimation by using WLS technique with white noise

Variable	Design value (full load)	Measurement value (50% load)	Simulation value by mathematical model (50% load)	Discrepancy (Simulation-measurement) %	Estimated value (50% load)	Discrepancy (Simulation-estimated) %
$T_{eci}\ ^oC$	248.000	212.800	213.500	0.328	212.585	0.429
$T_{eco}\ ^oC$	320.000	240.830	241.300	0.195	242.129	-0.343
$T_{ecm}\ ^oC$	323.000	243.350	242.458	-0.368	243.345	-0.366
$T_{geci}\ ^oC$	350.000	252.750	250.503	-0.897	251.857	-0.541
$T_{geco}\ ^oC$	480.000	332.500	326.706	-1.773	332.217	-1.687
$T_{drs}\ ^oC$	360.000	299.800	295.522	-1.447	296.504	-0.332
$T_{drw}\ ^oC$	345.000	282.576	286.576	1.396	286.283	0.102
$T_{wm}\ ^oC$	366.000	292.950	300.641	2.558	301.645	-0.333
$T_{pi}\ ^oC$	360.000	298.900	295.522	-1.143	296.504	-0.332
$T_{po}\ ^oC$	460.000	383.520	381.700	-0.477	384.536	-0.743
$T_{pm}\ ^oC$	468.000	392.214	387.645	-1.179	390.627	-0.769
$T_{s1i}\ ^oC$	420.000	351.090	349.705	-0.396	352.219	-0.719
$T_{s1o}\ ^oC$	512.000	468.323	466.500	-0.391	469.041	-0.544
$T_{s1m}\ ^oC$	518.000	471.547	475.481	0.827	478.022	-0.534
$T_{s2i}\ ^oC$	495.000	449.525	439.962	-2.174	442.286	-0.528
$T_{s2o}\ ^oC$	540.000	512.450	510.600	-0.362	509.823	0.152
$T_{s2m}\ ^oC$	548.230	523.658	527.518	0.732	525.659	0.352
$T_{ri}\ ^oC$	360.000	353.720	354.900	0.332	353.716	0.334
$T_{ro}\ ^oC$	540.000	512.650	509.800	-0.559	512.734	-0.576
$T_{rm}\ ^oC$	546.000	516.356	513.001	-0.654	516.276	-0.638
$P_{eci}\ bar$	160.000	93.730	94.230	0.531	93.668	0.596
$P_{eco}\ bar$	151.000	82.750	82.317	-0.526	83.301	-1.195

P_{dr} bar	150.000	81.955	80.993	-1.188	82.149	-1.427
P_{po} bar	147.700	80.550	79.263	-1.624	80.001	-0.931
P_{s1i} bar	144.800	78.850	77.082	-2.294	77.293	-0.274
P_{s1o} bar	143.000	74.850	75.728	1.159	75.612	0.153
P_{s2o} bar	140.000	72.452	73.471	1.387	72.811	0.898
P_{ri} bar	42.000	21.000	20.888	-0.536	21.000	-0.536
P_{ro} bar	40.000	18.340	19.417	5.546	18.341	5.547
M kg/sec	142.778	68.200	68.400	0.292	69.521	-1.639
M_r kg/sec	123.100	49.750	50.616	1.711	49.750	1.711
M_f kg/sec	10.556	5.250	5.550	5.405	5.248	5.441
M_a kg/sec	95.342	56.423	55.516	-1.633	56.326	-1.459
M_{sp} kg/sec	8.567	4.250	4.104	-3.558	4.171	-1.633

S_e=3.22, S_m=4.832, S_e / S_m =0.666

Table 2. state estimation by using WLS technique with one bad data

Variable	True value (full load)	Measurement value (50% load)	Simulation value (mathematical model)	Discrepancy (Simulation-measurement) %	Estimated value	Discrepancy (Simulation-estimated) %
T_{eci} ^oC	248.000	212.800	213.500	0.328	212.606	0.419
T_{eco} ^oC	320.000	240.830	241.300	0.195	242.137	-0.347
T_{ecm} ^oC	323.000	243.350	242.458	-0.368	243.352	-0.369
$T_{geci\ oC}$	350.000	252.750	250.503	-0.897	251.867	-0.545
T_{geco} ^oC	480.000	332.500	326.706	-1.773	332.251	-1.697
T_{drs} ^oC	360.000	299.800	295.522	-1.447	296.849	-0.449
T_{drw} ^oC	345.000	000.000	286.576	100	286.170	0.142
T_{wm} ^oC	366.000	292.950	300.641	2.558	301.991	-0.449
T_{pi} ^oC	360.000	298.900	295.522	-1.143	296.847	-0.448
T_{po} ^oC	460.000	383.520	381.700	-0.477	384.543	-0.745
T_{pm} ^oC	468.000	392.214	387.645	-1.179	390.613	-0.766
T_{s1i} ^oC	420.000	351.090	349.705	-0.396	352.227	-0.721
T_{s1o} ^oC	512.000	468.323	466.500	-0.391	469.041	-0.545
T_{s1m} ^oC	518.000	471.547	475.481	0.827	478.022	-0.534
T_{s2i} ^oC	495.000	449.525	439.962	-2.174	442.286	-0.528
T_{s2o} ^oC	540.000	512.450	510.600	-0.362	509.822	0.152
T_{s2m} ^oC	548.230	523.658	527.518	0.732	525.640	0.356
T_{ri} ^oC	360.000	353.720	354.900	0.332	353.716	0.334
T_{ro} ^oC	540.000	512.650	509.800	-0.559	512.734	-0.576
T_{rm} ^oC	546.000	516.356	513.001	-0.654	516.276	-0.638
P_{eci} bar	160.000	93.730	94.230	0.531	93.627	0.640
P_{eco} bar	151.000	82.750	82.317	-0.526	83.664	-1.636
P_{dr} bar	150.000	81.955	80.993	-1.188	82.557	-1.931
P_{po} bar	147.700	80.550	79.263	-1.624	80.284	-1.288
P_{s1i} bar	144.800	78.850	77.082	-2.294	77.418	-0.436
P_{s1o} bar	143.000	74.850	75.728	1.159	75.639	0.118
P_{s2o} bar	140.000	72.452	73.471	1.387	72.674	1.085
P_{ri} bar	42.000	21.000	20.888	-0.536	21.000	-0.536
P_{ro} bar	40.000	18.340	19.417	5.546	18.340	5.547

M kg/sec	142.778	68.200	68.400	0.292	69.575	-1.718
M_r *kg/sec*	123.100	49.750	50.616	1.711	49.750	1.711
M_f *kg/sec*	10.556	5.250	5.550	5.405	5.248	5.441
M_a *kg/sec*	95.342	56.423	55.516	-1.633	56.335	-1.475
M_{sp} *kg/sec*	8.567	4.250	4.104	-3.558	4.175	-1.730

S_e=3.439, S_m=4.192, S_e/S_e =0.820

Table 3. state estimation by using WLS technique with four bad data

Variable	True value (full load)	Measurement value (50% load)	Simulation value (mathematical model)	Discrepancy (Simulation-measurement) %	Estimated value	Discrepancy (Simulation-estimated) %
T_{eci} ^oC	248.000	212.800	213.500	0.328	212.469	0.483
T_{eco} ^oC	320.000	240.830	241.300	0.195	241.953	-0.271
T_{ecm} ^oC	323.000	260.000	242.458	-7.235	243.166	-0.292
T_{geci} ^oC	350.000	252.750	250.503	-0.897	251.676	-0.468
T_{geco} ^oC	480.000	332.500	326.706	-1.773	332.042	-1.633
T_{drs} ^oC	360.000	299.800	295.522	-1.448	296.050	-0.179
T_{drw} ^oC	345.000	270.000	286.576	5.784	286.425	0.053
T_{wm} ^oC	366.000	292.950	300.641	2.558	301.195	-0.184
T_{pi} ^oC	360.000	298.900	295.522	-1.143	296.050	-0.179
T_{po} ^oC	460.000	383.520	381.700	-0.477	384.522	-0.739
T_{pm} ^oC	468.000	392.214	387.645	-1.179	390.645	-0.774
T_{s1i} ^oC	420.000	351.090	349.705	-0.396	352.203	-0.714
T_{s1o} ^oC	512.000	468.323	466.500	-0.391	468.910	-0.517
T_{s1m} ^oC	518.000	471.547	475.481	0.827	477.879	-0.504
T_{s2i} ^oC	495.000	449.525	439.962	-2.174	442.160	-0.500
T_{s2o} ^oC	540.000	512.450	510.600	-0.362	511.625	-0.201
T_{s2m} ^oC	548.230	000.000	527.518	100	528.146	-0.119
T_{ri} ^oC	360.000	353.720	354.900	0.332	353.716	0.334
T_{ro} ^oC	540.000	512.650	509.800	-0.559	512.734	-0.576
T_{rm} ^oC	546.000	516.356	513.001	-0.654	516.276	-0.638
P_{eci} *bar*	160.000	93.730	94.230	0.531	93.674	0.590
P_{eco} *bar*	151.000	00.000	82.317	100	82.819	-0.610
P_{dr} *bar*	150.000	81.955	80.993	-1.188	81.613	-0.765
P_{po} *bar*	147.700	80.550	79.263	-1.624	79.630	-0.463
P_{s1i} *bar*	144.800	78.850	77.082	-2.294	77.129	-0.061
P_{s1o} *bar*	143.000	74.850	75.728	1.159	75.577	0.199
P_{s2o} *bar*	140.000	72.452	73.471	1.387	72.990	0.655
P_{ri} *bar*	42.000	21.000	20.888	-0.536	21.000	-0.536
P_{ro} *bar*	40.000	18.340	19.417	5.547	18.340	5.547
M kg/sec	142.778	68.200	68.400	0.292	69.588	-1.737
M_r *kg/sec*	123.100	49.750	50.616	1.711	49.750	1.711
M_f *kg/sec*	10.556	5.250	5.550	5.405	5.248	5.441
M_a *kg/sec*	95.342	56.423	55.516	-1.634	56.277	-1.371
M_{sp} *kg/sec*	8.567	4.250	4.104	-3.558	4.175	-1.730

S_e=2.872, S_m=4.259, S_e/S_m=0.674

Table 4. state estimation by using WLS technique with ten bad data

Variable	True value (full load)	Measurement value (50% load)	Simulation value (mathematical model)	Discrepancy (Simulation-measurement) %	Estimated value	Discrepancy (Simulation-estimated) %
$T_{eci}\ ^oC$	248.000	212.800	213.500	0.328	212.277	0.573
$T_{eco}\ ^oC$	320.000	240.830	241.300	0.195	241.516	-0.090
$T_{ecm}\ ^oC$	323.000	000.000	242.458	100%	242.721	-0.108
$T_{geci}\ ^oC$	350.000	000.000	250.503	100%	251.204	-0.280
$T_{geco}\ ^oC$	480.000	332.500	326.706	-1.773	331.373	-1.429
$T_{drs}\ ^oC$	360.000	299.800	295.522	-1.447	296.406	-0.299
$T_{drw}\ ^oC$	345.000	000.000	286.576	100%	286.296	0.098
$T_{wm}\ ^oC$	366.000	320.000	300.641	-6.439	301.556	-0.304
$T_{pi}\ ^oC$	360.000	298.900	295.522	-1.143	296.406	-0.299
$T_{po}\ ^oC$	460.000	383.520	381.700	-0.477	382.926	-0.321
$T_{pm}\ ^oC$	468.000	000.000	387.645	100	388.919	-0.329
$T_{s1i}\ ^oC$	420.000	351.090	349.705	-0.396	350.765	-0.303
$T_{s1o}\ ^oC$	512.000	468.323	466.500	-0.391	470.199	-0.793
$T_{s1m}\ ^oC$	518.000	000.000	475.481	100%	479.509	-0.847
$T_{s2i}\ ^oC$	495.000	449.525	439.962	-2.174	443.348	-0.77
$T_{s2o}\ ^oC$	540.000	512.450	510.600	-0.362	511.83	-0.241
$T_{s2m}\ ^oC$	548.230	000.000	527.518	100	527.99	-0.089
$T_{ri}\ ^oC$	360.000	353.720	354.900	0.332	353.716	0.334
$T_{ro}\ ^oC$	540.000	512.650	509.800	-0.559	512.734	-0.576
$T_{rm}\ ^oC$	546.000	516.356	513.001	-0.654	516.276	-0.638
P_{eci} *bar*	160.000	93.730	94.230	0.531	93.632	0.635
P_{eco} *bar*	151.000	00.000	82.317	100	83.193	-1.064
P_{dr} *bar*	150.000	81.955	80.993	-1.188	82.033	-1.284
P_{po} *bar*	147.700	71.000	79.263	10.425	80.095	-1.050
P_{s1i} *bar*	144.800	78.850	77.082	-2.294	77.652	-0.739
P_{s1o} *bar*	143.000	00.000	75.728	100	76.135	-0.537
P_{s2o} *bar*	140.000	72.452	73.471	1.387	73.608	-0.186
P_{ri} *bar*	42.000	21.000	20.888	-0.536	21	-0.536
P_{ro} *bar*	40.000	18.340	19.417	5.546	18.34	5.547
M kg/sec	142.778	68.200	68.400	0.292	69.741	-1.961
M_r *kg/sec*	123.100	49.750	50.616	1.711	49.75	1.711
M_f *kg/sec*	10.556	5.250	5.550	5.405	5.247	5.459
M_a *kg/sec*	95.342	56.423	55.516	-1.633	56.158	-1.156
M_{sp} *kg/sec*	8.567	4.250	4.104	-3.558	4.184	-1.949

S_e=2.999, S_m=3.119, S_e/S_m =0.961

5. Conclusions

The results proved that the weighted least squares algorithm adopted in this research is capable of detecting and identifying bad data of the boiler bad data. Four cases of data were considered and according to their deviation from the true value. As shown in the table (1) small deviations in the measured values, within the acceptable ranges, do not appear as bad data. The presence of bad data is taken by three cases, single bad data (zero reading) as appears in table 2, four bad data and ten bad data with different values as indicated in tables 3 and 4 respectively. This adopted approach is efficient in excluding bad data and replacing it with estimated values. The maximum number of zero reading that identified, removed and replaced with estimated values, was found to be 10. The obtained redundancy ratio with efficient estimation for Al-Doura power station was 2.125.

Acknowledgements

I would like to thank the staff of the Al-Doura thermal power station and its manager and the head of the training and development department, Mr. Hassan for helping me facilitate my task in taking the operational data of the station as well as providing me with the necessary information to complete the research.

Abbreviations

T_{eci}	Economizer temperature inlet (°C)	T_{s1i}	First bank secondary superheater temperature inlet (°C)
T_{eco}	Economizer temperature outlet (°C)	T_{s1o}	First bank secondary superheater temperature outlet (°C)
T_{ecm}	Economizer metal temperature (°C)	T_{s1m}	First bank secondary superheater metal temperature (°C)
T_{geci}	Economizer gas temperature inlet (°C)	T_{s2i}	Second bank secondary superheater temperature inlet (°C)
T_{geco}	Economizer gas temperature outlet (°C)	T_{s2o}	Second bank secondary superheater temperature outlet (°C)
T_{drs}	Drum steam temperature (°C)	T_{s2m}	Second bank secondary superheater metal temperature (°C)
T_{drw}	Drum water temperature (°C)	T_{ri}	Reheater temperature inlet (°C)
T_{wm}	Water wall metal temperature (°C)	T_{ro}	Reheater temperature outlet (°C)
T_{pi}	primary superheater temperature inlet (°C)	T_{rm}	Reheater metal temperature (°C)
T_{po}	primary superheater temperature outlet (°C)	P_{eci}	Pressure of economizer inlet (bar)
T_{pm}	primary superheater metal temperature (°C)	P_{eco}	Pressure of economizer outlet (bar)
P_{po}	Pressure of primary superheater outlet (bar)	P_{dr}	Pressure of drum (bar)
P_{s1i}	Pressure of first bank secondary superheater inlet (bar)	H_{pi}	Primary superheater enthalpy inlet (kJ/kg)
P_{s1o}	Pressure of first bank secondary superheater outlet (bar)	H_{po}	Primary superheater enthalpy outlet (kJ/kg)
P_{s2o}	Pressure of second bank secondary superheater outlet (bar)	C_{pi}	Specific heat of primary superheater steam inlet (kJ/kg°C)
P_{ri}	Pressure of reheater inlet (bar)	C_{po}	Specific heat of primary superheater steam outlet (kJ/kg°C)
P_{ro}	Pressure of reheater outlet (bar)	K_{p1}	Heat transfer coefficient at the steam side of the primary superheater tubes (kW/°C)
M	Steam mass flow rate (kg/s)	H_{s1i}	First bank secondary superheater enthalpy inlet (kJ/kg)
M_r	Reheat mass flow rate (kg/s)	H_{s1o}	First bank secondary superheater enthalpy outlet (kJ/kg)
M_g	Gas mass flow rate (kg/s)	C_{s1i}	Specific heat of first bank secondary superheater steam inlet (kJ/kg°C)
H_{eci}	Economizer enthalpy inlet (kJ/kg)	C_{s1o}	Specific heat of first bank secondary

			superheater steam outlet (kJ/kg°C)
H_{eco}	Economizer enthalpy outlet (kJ/kg)	K_{s11}	Heat transfer coefficient at the steam side of 1st bank secondary superheater tubes (kW/°C)
C_{eci}	Specific heat of economizer water inlet (kJ/kg°C)	H_{s2i}	Second bank secondary superheater enthalpy inlet (kJ/kg)
C_{eco}	Specific heat of economizer water outlet (kJ/kg°C)	H_{s2o}	Second bank secondary superheater enthalpy outlet (kJ/kg)
K_{ec1}	Heat transfer coefficient at the water side of the economizer tubes (kW/°C)	C_{s2i}	Specific heat of second bank secondary superheater steam inlet (kJ/kg°C)
K_{ec2}	Heat transfer coefficient at the gas side of the economizer tubes (kW/°C)	C_{s2o}	Specific heat of second bank secondary superheater steam outlet (kJ/kg°C)
C_{gec}	Specific heat of gas at economizer side (kJ/kg°C)	K_{s21}	Heat transfer coefficient at the steam side of 2nd bank secondary superheater tubes (kW/°C)
H_{drs}	Saturated steam enthalpy in drum (kJ/kg)	H_{ri}	Reheater enthalpy inlet (kJ/kg)
H_{drw}	Saturated water enthalpy in drum (kJ/kg)	H_{ro}	Reheater enthalpy outlet (kJ/kg)
ρ_{wos}	Saturated steam density in drum (kg/m^3)	C_{ri}	Specific heat of reheater steam inlet (kJ/kg°C)
ρ_{wow}	Saturated water density in drum (kg/m^3)	C_{ro}	Specific heat of reheater steam outlet (kJ/kg°C)
C_{drw}	Specific heat of drum water (kJ/kg°C)	K_{r1}	Heat transfer coefficient at the steam side of the reheater tubes (kW/°C)
K_{w1}	Heat transfer coefficient at the water side of the water wall tubes (kW/°C)		

References

[1] G. F. M. De Souza, *Thermal power plant performance analysis*. Springer, 2012.

[2] A. Assefinejad, A. Kermanpur, and A. Eslami, "A semi-analytical approach on critical thermal states in water wall tubes of a subcritical drum boiler of a thermal power plant," *International Journal of Pressure Vessels and Piping*, vol. 194, p. 104507, 2021.

[3] Z.-C. Guan, X. Liu, W.-D. Jiao, and X.-C. Zhang, "Research on the Application of Intelligent Control in Thermal Automation of Thermal Power Plants," *Engineering Technology Trends*, vol. 2, no. 5, 2024.

[4] A. Sumalatha, K. S. Rani, and C. Jayalakshmi, "Dynamic modeling of Boiler drum using nonlinear system identification approach," *Measurement: Sensors*, vol. 28, p. 100845, 2023.

[5] Y. Wang *et al.*, "A novel thermodynamic method and insight of heat transfer characteristics on economizer for supercritical thermal power plant," *Energy*, vol. 191, p. 116573, 2020.

[6] S. Agbleze, L. J. Shadle, and F. V. Lima, "Dynamic Modeling and Simulation of a Subcritical Coal-Fired Power Plant under Load-Following Conditions," *Industrial & Engineering Chemistry Research*, 2024.

[7] K. Lo, Z. Song, E. Marchand, and A. Pinkerton, "Development of a static-state estimator for a power station boiler Part II. Estimation algorithm and bad data processing," *Electric power systems research*, vol. 18, no. 3, pp. 191-203, 1990.

[8] K. Lo, P. Zeng, E. Marchand, and A. Pinkerton, "Modelling and state estimation of power plant steam turbines," in *IEE Proceedings C (Generation, Transmission and Distribution)*, 1990, vol. 137, no. 2: IET, pp. 80-94.

[9] C. E. Bandak, "Power systems state estimation," 2013.

[10] T. Vishnu, V. Viswan, and A. Vipin, "Power system state estimation and bad data analysis using weighted least square method," in *2015 International Conference on Power, Instrumentation, Control and Computing (PICC)*, 2015: IEEE, pp. 1-5.

[11] M. Majdoub *et al.*, "Study of state estimation using weighted least squares method," *Int. J. Adv. Eng. Res. Sci.(IJAERS)*, vol. 3, no. 8, 2016.

[12] A. Jovicic and G. Hug, "Linear state estimation and bad data detection for power systems with RTU and PMU measurements," *IET Generation, Transmission & Distribution*, vol. 14, no. 23, pp. 5675-5684, 2020.

[13] A. N. Putri, O. Penangsang, and M. A. H. Sirad, "Power Flow Based Monitoring Of State Estimation Using The Weighted Least Square," in *2020 International Seminar on Application for Technology of Information and Communication (iSemantic)*, 2020: IEEE, pp. 408-411.

[14] A. Airoboman, I. Araga, and I. Afolayan, "STATE ESTIMATION OF THE NIGERIAN 330KV TRANSMISSION NETWORK USING THE WEIGHTED LEAST SQUARE OPTIMIZATION TECHNIQUE," vol. 17, pp. 495-504, 12/29 2021.

[15] L. Kumar and P. K. Kherdikar, "An overview of different static state estimation techniques with bad data detection, identification and elimination in power system," *International Journal of Ambient Energy*, vol. 43, no. 1, pp. 4305-4309, 2022.

[16] A. Hondo, E. Begić, and T. Hubana, "State Estimation in Electric Power Systems Using Weighted Least Squares Method," 2023, pp. 595-605.

[17] C. Sheikh, "Power System State Estimation using Weighted Least Square Method," *Proceeding International Conference on Science and Engineering*, vol. 11, pp. 1721-1727, 02/18 2023, doi: 10.52783/cienceng.v11i1.327.

[18] K. Lo, Z. Song, E. Marchand, and A. Pinkerton, "Development of a static-state estimator for a power station boiler Part I. Mathematical model," *Electric power systems research*, vol. 18, no. 3, pp. 175-189, 1990.

[19] H. Kwan and J. Anderson, "A mathematical model of a 200 MW boiler," *International Journal of control*, vol. 12, no. 6, pp. 977-998, 1970.

[20] P. B. Usoro, "Modeling and simulation of a drum boiler-turbine power plant under emergency state control," Massachusetts Institute of Technology, 1977.

[21] P. T. Nicholson, "Boiler-turbine modelling and simulation," UNSW Sydney, 1983.

[22] E. E. Fetzer and P. Anderson, "Observability in the state estimation of power systems," *IEEE transactions on power Apparatus and Systems*, vol. 94, no. 6, pp. 1981-1988, 1975.

[23] A. Abur and A. G. Exposito, *Power system state estimation: theory and implementation*. CRC press, 2004.

[24] M. R. J. Motiyani, A. R. Chudasama, and M. A. P. Desai, "ELECTRICAL POWER SYSTEM STATE ESTIMATION: THEORY AND IMPLEMENTATION," 2015.

[25] F. Broussolle, "State estimation in power systems: Detecting bad data through the sparse inverse matrix method," *IEEE Transactions on Power Apparatus and Systems*, no. 3, pp. 678-682, 1978.

Appendix – A

$h_{(1,1)} = 1$ $\quad$ $h_{(1,2)} = 0$

$h_{(2,1)} = 0$ $\quad$ $h_{(2,2)} = 1$

$h_{(3,1)} = -\frac{C_{eci}M^{0.2}}{K_{ec1}}$ $\quad$ $h_{(3,2)} = (1 + \frac{C_{eco}M^{0.2}}{K_{ec1}})$

$h_{(3,13)} = -\frac{0.2C_{eci}}{K_{ec1}M^{0.8}} T_{eci} + (\frac{0.2C_{eco}}{K_{ec1}M^{0.8}}) T_{eco} = \frac{0.2}{K_{ec1}M^{0.8}} (C_{eco} T_{eco} - C_{eci} T_{eci})$

$$h_{(4,1)} = -C_{eci}\left(\frac{M}{K_{ec2}M_g^{0.6}} + \frac{M^{0.2}}{K_{ec1}}\right)$$

$$h_{(4,2)} = 1 + C_{eco}M\left(\frac{1}{K_{ec2}M_g^{0.6}} + \frac{1}{K_{ec1}M^{0.8}}\right) = 1 + C_{eco}\left(\frac{M}{K_{ec2}M_g^{0.6}} + \frac{M^{0.2}}{K_{ec1}}\right)$$

$$h_{(4,13)} = -C_{ei}\left(\frac{1}{K_{ec2}M_g^{0.6}} + \frac{0.2}{K_{ec1}M^{0.8}}\right)T_{eci} + C_{eo}\left(\frac{1}{K_{ec2}M_g^{0.6}} + \frac{0.2}{K_{ec1}M^{0.8}}\right)T_{eco}$$

$$= \left(\frac{1}{K_{ec2}M_g^{0.6}} + \frac{0.2}{K_{ec1}M^{0.8}}\right)\left(C_{eco}T_{eco} - C_{eci}T_{eci}\right)$$

$$h_{(4,15)} = \left(\frac{0.6M}{K_{ec2}M_g^{1.6}}\right)\left(C_{eci}T_{eci} - C_{eco}T_{eco}\right)$$

$$h_{(4,16)} = \left(\frac{0.6M}{K_{ec2}M_g^{1.6}}\right)\left(C_{eci}T_{eci} - C_{eco}T_{eco}\right)$$

$$h_{(5,1)} = -C_{eci}M\left(\frac{1}{C_{gec}M_g} + \frac{1}{K_{ec2}M_g^{0.6}} + \frac{1}{K_{ec1}M^{0.8}}\right)$$

$$h_{(5,2)} = 1 + C_{eco}M\left(\frac{1}{C_{gec}M_g} + \frac{1}{K_{ec2}M_g^{0.6}} + \frac{1}{K_{ec1}M^{0.8}}\right)$$

$$h_{(5,13)} = -C_{eci}\left(\frac{1}{C_{gec}M_g} + \frac{1}{K_{ec2}M_g^{0.6}} + \frac{0.2}{K_{ec1}M^{0.8}}\right)T_{eci} + C_{eco}\left(\frac{1}{C_{gec}M_g} + \frac{1}{K_{ec2}M_g^{0.6}} + \frac{0.2}{K_{ec1}M^{0.8}}\right)T_{eco}$$

$$= \left(\frac{1}{C_{gec}M_g} + \frac{1}{K_{ec2}M_g^{0.6}} + \frac{0.2}{K_{ec1}M^{0.8}}\right)\left(C_{eco}T_{eco} - C_{eci}T_{eci}\right)$$

$$h_{(5,15)} = C_{eci}M\left(\frac{1}{C_{gec}M_g^{2}} + \frac{0.6}{K_{ec2}M_g^{1.6}}\right)T_{eci} - C_{eco}M\left(\frac{1}{C_{gec}M_g^{2}} + \frac{0.6}{K_{ec2}M_g^{1.6}} +\right)T_{eco}$$

$$= M\left(\frac{1}{C_{ge}M_g^{2}} + \frac{0.6}{K_{e2}M_g^{1.6}}\right)\left(C_{eci}T_{eci} - C_{eco}T_{eco}\right)$$

$$h_{(6,9)} = 2A_1P_{dr} + B_1$$

$$h_{(7,2)} = \frac{xC_{eco}}{C_{drw}}$$

$$h_{(7,9)} = \frac{(1-x)}{C_{drw}}(2A_2P_{dr} + B_2)$$

$$h_{(7,13)} = \frac{1}{C_{drw}*M_w}\left(C_{eco}T_{eco} - H_{drs}\right)$$

$$h_{(8,2)} = \frac{MC_{eco}}{3K_w}\left(\frac{M(H_{drs} - C_{eco}T_{eco})}{K_w}\right)^{\frac{-2}{3}} = \left(-\frac{C_{eco}M^{\frac{1}{3}}}{\frac{1}{3K_w^{3}(H_{drs}-C_{eco}T_{eco})^{\frac{2}{3}}}}\right)$$

$$h_{(8,9)} = \left(\frac{2M^{\frac{1}{3}}}{3K_w^{\frac{1}{3}}(H_{drs} - C_{eco}T_{eco})^{\frac{2}{3}}}\right)(A_2P_{dr} + B_2) + (2A_1P_{dr} + B_1)$$

$$h_{(8,13)} = \frac{(H_{drs}-C_{eco}T_{eco})^{3^{\frac{1}{}}}}{3K_w^{\frac{1}{3}}M^{\frac{2}{3}}}$$

$$h_{(9,9)} = 2A_1P_{dr} + B_1 \qquad h_{(10,3)} = 1$$

$$h_{(11,3)} = \left(1 + \frac{C_{po}M^{0.2}}{K_{p1}}\right)$$

$$h_{(11,9)} = -\left(\frac{C_{pi}M^{0.2}}{K_{p1}}\right)(2A_1P_{dr} + B_1)$$

$h_{(11,13)} = \frac{0.2}{K_{p1}\, M^{0.8}} (C_{po} T_{po} - C_{pi} T_{pi})$

$h_{(12,1)} = \frac{M_{sp1} C_{eci}}{(M + M_{sp1}) C_{s1i}}$

$h_{(12,3)} = \frac{M C_{po}}{(M + M_{sp1}) C_{s1i}}$

$h_{(12,13)} = 0 \qquad h_{(13,4)} = 1$

$h_{(14,1)} = - \frac{C_{eci} M_{sp}}{K_{s11} (M + M_{sp})^{0.8}}$

$h_{(14,3)} = - \frac{C_{po} (M + M_{sp})^{0.2}}{K_{s11}}$

$h_{(14,4)} = 1 + \frac{C_{slo} (M + M_{sp1})^{0.2}}{K_{s11}}$

$h_{(14,13)} = [\frac{1}{K_{s11} (M + M_{sp1})^{0.8}} (0.2 C_{s1o} T_{s1o} - C_{po} T_{po}) + \frac{0.8}{K_{s11} (M + M_{sp1})^{1.8}} (M_{sp1} C_{eci} T_{eci} + M C_{po} T_{po})]$

$h_{(15,1)} = \frac{M_{sp2} C_{eci}}{(M_{s1} + M_{sp}) C_{s2i}}$

$h_{(15,4)} = \frac{M_{s1} C_{s1o}}{(M_{s1} + M_{sp2}) C_{s2i}}$

$h_{(15,13)} = 0 \qquad h_{(16,5)} = 1$

$h_{(17,1)} = - \frac{C_{eci} M_{sp2}}{K_{s21} (M_{s1} + M_{sp1})^{0.8}}$

$h_{(17,4)} = - \frac{C_{s1o} (M_{s1} + M_{sp1})^{0.2}}{K_{s21}}$

$h_{(17,5)} = 1 + \frac{C_{s1o} (M_{s1} + M_{sp1})^{0.2}}{K_{s21}}$

$h_{(17,13)} = [\frac{1}{K_{s21} (M_{s1} + M_{sp1})^{0.8}} (0.2 C_{s2o} T_{s2o} - C_{s1o} T_{s1o}) + \frac{0.8}{K_{s21} (M_{s1} + M_{sp1})^{1.8}} (M_{sp1} C_{eci} T_{eci} + M_{s1} C_{s1o} T_{s1o})]$

$h_{(18,6)} = 1 \qquad h_{(19,7)} = 1$

$h_{(20,6)} = - \frac{C_{ri} M_r^{0.2}}{K_{r1}}$

$h_{(20,7)} = (1 + \frac{C_{ro} M_r^{0.2}}{K_{r1}})$

$h_{(21,8)} = 1 \qquad h_{(22,8)} = 0.1$

$h_{(22,9)} = 0.9 \qquad h_{(23,9)} = 1$

$h_{(24,9)} = 0.77 \qquad h_{(24,10)} = 0.23$

$h_{(25,9)} = 0.48 \qquad h_{(25,10)} = 0.52$

$h_{(26,9)} = 0.3 \qquad h_{(26,10)} = 0.7$

$h_{(27,10)} = 1 \qquad h_{(28,11)} = 1$

$h_{(29,12)} = 0.66$ $h_{(30,13)} = 0.34$

$h_{(31,14)} = 1$ $h_{(32,15)} = 1$ $h_{(33,16)} = 1$ $h_{(34,13)} = 0.06$

Appendix – B

Table 5. specific heat at the inlet and outlet of each section under full load conditions (k J/ kg °C)

C_{eci}	4.338	C_{s1o}	6.545
C_{eco}	4.567	C_{s2i}	6.681
C_{pi}	6.892	C_{s2o}	6.355
C_{po}	6.928	C_{ri}	8.645
C_{s1i}	7.284	C_{ro}	6.550
C_{drw}	8.675		

Table 6. Heat transfer coefficients (KW/C)

K_{ec1}	346.7097	K_{s21}	43.003
K_{ec2}	124.314	K_{r1}	185.3894
K_{p1}	237.958	K_{wr1}	751.018
K_{s11}	132.699		

Table 7. Drum pressure relationship constant $140 \leq Pdr \leq 200\ bar$

	1	2	3	4	5
A	-0.0012	-0.0264	0.0095	0.0109	-0.0099
B	0.8944	5.2427	0.9981	-2.317	1.2324
C	235.23	2419.8	1247.2	199.11	641.18

Table 8. Drum pressure relationship constant $70 \leq Pdr \leq 130\ bar$

	1	2	3	4	5
A	-0.003	-0.0068	-0.0097	0.0021	0.0008
B	1.3389	-0.0458	6.149	0.2666	-1.8519
C	206.76	2617	875.12	7.487	865.87